Journal of Photochemistry and Photobiology A: Chemistry 208 (2009) 66–77

Contents lists available at ScienceDirect

Journal of Photochemistry and Photobiology A: Chemistry

journal homepage: www.elsevier.com/locate/jphotochem

Effects of hydroxyl radicals and oxygen species on the 4-chlorophenol degradation by photoelectrocatalytic reactions with TiO_2-film electrodes

Juan Yang[a,*], Jun Dai[a], Chuncheng Chen[b], Jincai Zhao[b]

[a] Department of Physical Chemistry, Henan Polytechnic University, Jiaozuo 454003, Henan, China
[b] Beijing National Laboratory for Molecular Sciences, Institute of Chemistry, The Chinese Academy of Sciences, Beijing 100080, China

ARTICLE INFO

Article history:
Received 11 January 2009
Received in revised form 5 June 2009
Accepted 25 August 2009
Available online 31 August 2009

Keywords:
TiO_2-film electrode
Oxygen species
H_2O^{18}
Mineralization
4-CP

ABSTRACT

The supported nano-TiO_2 electrode was prepared by sol–gel and hydrothermal method, and the photoelectrocatalytic degradation of 4-chlorophenol (4-CP) under UV irradiation has been investigated to reveal the roles of hydroxyl radicals and dissolved oxygen species for TiO_2-assisted photocatalytic reactions. The degradation kinetics, the formation and decay of intermediates, the isotopic tracer experiments with H_2O^{18}, the removal yield of total organic carbon and the formation of active radical species in the presence of oxygen or not were examined by HPLC, GC–MS, TOC and spin-trap ESR spectrometry. It was found that most of •OH radicals in the primary hydroxylated intermediates derived from the oxidation of adsorbed H_2O or HO^- by photo-holes in the electrochemically assisted TiO_2 photocatalytic system. It also indicates that the enhancement in the separation efficiency of photogenerated charges by applying a positive bias (+0.5 V *vs* SCE) has little role in the following decomposition and mineralization of these hydroxylated intermediates in the absence of oxygen. According to above experimental results, the pathway of 4-CP photocatalytic degradation was deduced initially. Due to the combined effect of •OH radicals and dissolved oxygen species, the hydroxylated 4-chlorphenol, via *cis, cis*-3-chloromuconic acid, was decomposed into low molecular weight acid and CO_2.

1. Introduction

TiO_2-based photocatalysis has gained much attention in its chemical utilization, albeit somewhat limited, of inexpensive and inexhaustible solar radiation toward environmental detoxification. The primary events occurring on UV-illuminated TiO_2 relative to the photodegradation of organic pollutants are summarized in Scheme 1. Absorption of the near-UV light by TiO_2 at wavelengths $\lambda < 385$ nm is followed by electron (e^-)–hole (h^+) pair generation (Eq. (1)). These charge carriers can migrate rapidly to the surface of catalyst particles where they are ultimately trapped and poised to undergo redox chemistry with suitable substrates. Thus, the trapped hole can react with surface adsorbed organic contaminant to produce organic radical cation (Eq. (2)) or with chemisorbed OH^- or H_2O to produce •OH radicals (Eq. (3)) [1–3]. In aerated systems, dioxygen acts as an efficient electron scavenger to trap the conduction band electron to yield superoxide radical anions $O_2^{\bullet -}$ (Eq. (4)) [1–3]. In acidic solution, superoxides $O_2^{\bullet -}$ can be protonated to form the hydroperoxyl radical HOO• (Eq. (5)), following by doubly scavenging photo-electrons and generating H_2O_2 (Eq. (6)) and •OH radicals (Eq. (7)) [3–5]. Evidently, •OH radicals formed in TiO_2 photocatalysis derive from two different approaches, that is, oxidation chemisorbed OH^- or H_2O by photo-holes and reduction dissolved O_2 by photoelectrons.

In spite of experimental results or theoretical calculations for TiO_2 photocatalysis, hydroxylation is regarded as the primary process in the degradation of aromatic contaminants, such as benzene, phenol and substituted phenol [6–9]. The generation of hydroxylated intermediates is mainly attributed to the aryl addition with surface •OH radicals [8–11] formed in the photocatalytic primary steps. However, the origination of these hydroxyl radicals remains rather controversial. Besides two mechanisms about the formation of •OH radicals mentioned (Eqs. (3) and (7)), recent reports have shown that •OH radicals, the active species in primary oxidizing reactions, were formed by photo-hole oxidating of surface oxygen ions at a terminal lattice O site [12,13]. Moreover, most of the previous studies have ascribed almost all process to hydroxyl radical chemistry, including the hydroxylation of unsubstituted aryl positions and their mineralization under UV irradiation, but neglected the roles of dissolved oxygen and related species. Therefore, the obtained conclusions are incomplete and unconvincing. A better understanding of the basic mechanism involved is a first step in the overall improvement of the efficiency of photodegradation of organic pollutants.

* Corresponding author. Tel.: +86 391 3989667; fax: +86 391 3987058.
E-mail address: yangjuan0302@yahoo.cn (J. Yang).

1010-6030/$ – see front matter © 2009 Elsevier B.V. All rights reserved.
doi:10.1016/j.jphotochem.2009.08.007

$$TiO_2 \xrightarrow{h\nu} e^-_{CB} + h^+_{VB} \quad \text{charge separation} \tag{1}$$

$$h^+_{VB} + RH \longrightarrow R^{\bullet +} + H^{\bullet} \tag{2}$$

$$h^+_{VB} + H_2O_{ads} / OH^- \longrightarrow {}^{\bullet}OH_{ads}(a) + (H^+_{ads}) \tag{3}$$

$$e^-_{CB} + O_{2ads} \longrightarrow O^{\bullet -}_{2ads} \tag{4}$$

In acidic solution, the following process takes also place:

$$O^{\bullet -}_2 + H^+ \longrightarrow HO^{\bullet}_2 \tag{5}$$

$HO^{\bullet}_2$ being another oxidative species involved in the following processes in which it forms H_2O_2 and $^{\bullet}OH$:

$$HO^{\bullet}_{2ads} + H^+_{ads} + e^- \longrightarrow H_2O_{2ads} \tag{6}$$

$$H_2O_{2ads} + e^-_{ads} \longrightarrow {}^{\bullet}OH_{ads}(b) + OH^-_{ads} \tag{7}$$

$$\text{pollutants} + {}^{\bullet}OH_{ads}(a) / {}^{\bullet}OH_{ads}(b) \longrightarrow \text{hydroxylated products} \tag{8}$$

Scheme 1. Primary process involved in TiO_2 photocatalysis.

Mostly, the photocatalytic degradation reactions are carried out in presence of water, air, TiO_2 and target contaminants. In such suspensions, there is a great handicap to unveil the different roles of radical species since all the reactions take place on the same particle. It is of importance, hence, to separate the formation and reaction of different radicals with each other. To this end, the photoelectrochemistry by TiO_2-film electrode seems to provide an ideal method for the mechanistic investigation of photocatalysis since Fujishima and Honda [14] first achieved charge separation with an electrochemical bias. In this system, when applied a positive bias on TiO_2-film electrode, photogenerated electrons in the excited TiO_2-film anode are taken away via the external circuit, instead of the electron transfer to molecular oxygen in suspension system, and consequently, the photogenerated hole or $^{\bullet}OH$ is left at the surface of the TiO_2 electrode. Therefore, it is possible to improve the efficiency of oxidation at the semiconductor–electrolyte interface. Although many researchers have paid attention to the photoelectrochemical methods for the degradation of the organic pollutants under UV irradiation [15–21], their fundamental aims were merely to enhance photogenerated electron/hole separation by an applied potential bias. The photoelectrochemical degradation mechanism has also been examined in these studies. However, most of them have only emphasized the enhancement in the formation of $^{\bullet}OH$ radicals, and their roles for the degradation of organic pollutants. Most importantly, in the photoelectrocatalytic system, it can be realized facilely that large quantities of $^{\bullet}OH$ radicals exist by using a positive bias, even if in absence of dissolved oxygen. As a result, the photoelectrochemistry provides a powerful and desirable method to research the roles of different radical species individually.

Chlorocarbons in aqueous solutions like 4-CP have been recognized as a threat to human health by both the EU (European Union) and US EPA (United State Environmental Protection Agency) [22], and a comprehensive review by Esplugas and co-workers has appeared referencing the studies to abate this compound by TiO_2 photocatalysis [23]. Our previous laboratory has also reported the degradation of 2,4-dichlorophenol by TiO_2 and POM/TiO_2 under UV irradiation [24].

In this study, we highlight the photoelectrochemical method on the application for the investigation of photocatalytic mechanism of the degradation of aromatic pollutants under UV irradiation. By using TiO_2 film prepared on TCO glass as a working electrode, the photoelectrocatalytic degradation of 4-CP was investigated by examination the primary hydroxylation and the following mineralization. Our experimental results indicate unambiguously that (a) the initial oxidative $^{\bullet}OH$ radical is mainly generated by photohole oxidation of TiO_2 surface hydroxyl ion and adsorbed H_2O; (b) the hydroxylated 4-chlorphenol, *via* 3-chloromuconic acid, was decomposed into low molecular weight acid and CO_2 is likely the main degradation pathway; (c) dissolved oxygen has an important role in the following oxidation and mineralization of the intermediates of 4-chlorophenol.

2. Experimental

2.1. Materials

Conducting glass sheets (<20 Ω/square, Lanbao Technologies Limited, transparent conductive oxide coated glass plates of fluorine-doped SnO_2) were employed as substrates for TiO_2 film coating. Titanium isopropoxide was obtained from Aldrich Chemical Co. Spin trap ping reagent 5,5-dimethyl-1-pyrroline-*N*-oxide (DMPO) was purchased from the Sigma Chemical Co. H_2O^{18} was received from Jiangsu Changshu Chemical Limited, which initial isotopic enrichment was 85.6% as determined by mass spectrometry. Glycolic acid, maleic acid, succinic acid, fumaric acid, malic acid, 1,1,1,3,3,3-hexamethyldisilazane (HMDS), chlorotrimethylsilane (TMSCl) and anhydrous pyridine were purchased from J&K Chemical Ltd. and used as received. Catechol, hydroquinone, benzoquinone, 4-chlorophenol, oxalic acid, malonic acid, 4-chlorocatechol, 4-chlororesorcinol and all other chemicals were of analytical reagent grade and used without further purification. Deionized and doubly distilled water was used throughout this study. The pH of the solutions was adjusted with dilute aqueous solutions of $HClO_4$ and NaOH.

2.2. Degradations

The photoelectrocatalytic degradation experiments were performed in a two-compartment reactor and standard three-

electrode mode. A porosity glass frit was used to separate the two compartments while allowing electrolyte (0.1 M Na_2SO_4) to permeate. The electrodes consisted of a polycrystalline TiO_2 working electrode, a Pt foil ($0.5 \times 4\,cm^2$) counter electrode and a saturated calomel electrode (SCE) as reference. TiO_2 film electrode was prepared according to the method described in our earlier study [25]. The cell was sealed with rubber stopples in the gas-sparging experiments. The photoactive area of the TiO_2 electrode was 6 cm^2. The reference electrode and counter electrode were separated from the working electrode and not exposed to illumination. A potentiostat model DJS-292 was used to bias the TiO_2 electrode and to measure the photoelectrochemical parameters. Irradiations were carried out using a 100 W high-pressure mercury lamp equipped with a cutoff filter (330 nm < λ < 400 nm).

2.3. HPLC analysis of kinetics

Kinetic runs were analyzed by HPLC and the initial concentration was 200 μM. Samples of approximately 0.5 mL were taken out before photolysis and at regular intervals during the irradiation. The concentrations of 4-CP and their hydroxylated products were measured by HPLC using a Dionex HPLC with a UVD 340S diode-array detector and a Dionex P580 pump. Substances were routinely quantified from their absorbance at 280 nm. The eluent was 55% aqueous methanol and 45% phosphate buffer solution (0.1%, v/v). The identification of the intermediates by HPLC was preformed by comparing the retention times and UV spectra with those of standards.

2.4. GC–MS analysis and identification of peaks in Table 1

After reactions were stopped, the solution (50 mL) was concentrated to 1 mL under reduced pressure. Water was removed by freezing-drying. The resulting material was treated with 0.1 mL of anhydrous pyridine, 0.1 mL of HMDS and 0.05 mL of TMSCl. The reaction was carried out in a 1.0 mL plastic centrifugal tube. The mixture was shaken vigorously for about 1 min and was then allowed to stand for 10 min at room temperature. Precipitate was separated by centrifugation and the silylated products were analyzed by GC–MS [26]. GC–MS analyses were carried out on a Finnigan Trace GC ultra gas chromatograph using a 25 m DB-5 column, coupled with a Finnigan Trace DSQ mass spectrometer. The injector port was set for split operation at 250 °C. The temperature program of the column was as follows: at 50 °C, hold time = 5 min; from 50 to 200 °C, rate = 10 °C/min. Most of the compounds whose TMS derivatives correspond to peaks in Table 1 were commercially available. These compounds were obtained and subjected to the silylation and GC/MS analysis as indicated above.

The preparation of peak 12 [27]. To a magnetically stirred solution of 5 mL of HOAc, 3.85 mL of 32% HOOAc, and 1 mg of ferric acetate was added, at a rate of approximately 1 drop per minute over about 5 h, 10 mL of a HOAc solution containing 5 mmol of 4-chlorocatechol. After complete addition, the reaction mixture was stirred for an additional 24 h at room temperature. The resulting suspension was then concentrated in vacuo, without heating. After the solution was cooled to 0–4 °C, the product was collected by suction filtration and washed with ice-cold water until the filtrate was colorless. Drying in vacuum over KOH yielded *cis*, *cis*-3-chloromuconic acid. ^{1}H NMR (400 MHz, acetone-d^6): δ 6.81 ppm (d, J11.7 Hz, 1H), 6.18 ppm (d, J11.6 Hz, 1H), 6.0 ppm (d, J11.6 Hz, 1H). ^{13}C NMR (300 MHz): δ 170.6, 170.2, 151.1, 145.4, 117.4 and 114.8 ppm. Mass spectrum of its TMS derivative (peak12): *m*/*z* (relative abundance), 73 (100), 147 (98), 203 (70), 205 (24), 285 (50), 305 (20) and 307 (7). HR-FAB-MS analysis for ion $C_6H_4O_4Cl^-$: 174.9803770, the calculated mass: 174.9803565 (error was only 1.173×10^{-7}).

2.5. General instrumentation

The surface morphology and crystal composition of the anodic TiO_2 films were examined by the S-4300F field-emission scanning electron microscopy (FESEM) and Rigaku D/max-2500 X-ray diffraction measurement (XRD). Total organic carbon was measured by a Tekmar Dohrmann Apollo 9000 TOC analyzer. The concentration of the chloride ions produced was determined using a chloride ion selective electrode under both static and dynamic conditions. The K_2HPO_4 was used for the buffer solution and to adjust the ionic strength. The electron spin resonance (ESR) signals of radicals trapped by DMPO were detected at ambient temperature on a Bruker (E 500) spectrometer. The irradiation source was the same as used in the degradation of 4-CP. The settings for the ESR spectrometer were as follows: center field, 3443 G; sweep width, 100 G; microwave frequency, 9.64 GHz; modulation frequency, 100 kHz; power, 10.05 mW.

3. Results and discussion

3.1. Characterization of nano-TiO_2 film

The morphology of TiO_2 film was examined by SEM and its image was shown in Fig. 1A. It can be seen that the nano-film uniformly consisted of TiO_2 particles of about 30–40 nm in diameter. The thickness was about 2 μm (inset in Fig. 1A). The XRD pattern of the nano-TiO_2 film calcined at 450 °C was analyzed, as shown in Fig. 1B. The TiO_2 film had characteristic peaks at 25.32° (1 0 1), 37.58° (1 0 1), 47.95° (2 0 0), 53.80° (2 1 1), and 62.67° (2 2 0), respectively. According to the XRD indexation, the crystal form of TiO_2 film was mainly anatase phase in good agreement with previous reports [25]. In addition, the quantity of TiO_2 loading was about 0.5 mg/cm^2 on average. From the SEM and XRD results, it can be confirmed that the TiO_2 nano-particles well spread on the conductive glass substrate successfully during the sol–gel and hydrothermal process.

3.2. Photoelectrochemical degradation of 4-CP

In the photoelectrochemical cell, the choice of bias potential is a critical factor for the removal of organic contaminations. The better result can be obtained when an appropriate bias is used. The photocurrent associated with the photoelectrode as a function of applied potential was investigated by recording linear sweep voltammetry curves. Fig. 2 shows the profile of these curves, as well as the dark current. As can be seen, under UV illumination the TiO_2 photoelectrode produced a photocurrent in 0.1 M Na_2SO_4 (pH ≈ 5.8) at −0.6 V *vs* SCE. This profile was expected, for the application of potentials higher than the TiO_2 flat band potential across a photoelectrode increases the concentration of photogenerated holes or hydroxyl radicals formed by subsequent oxidation of water on the surface and decreases the recombination rate of photogenerated holes and electrons [28]. As a result, the photocurrent was enhanced as the potential increases, improving the oxidative degradation process. In addition, curve b in Fig. 2 indicated that the photocurrent was enhanced evidently when the potential increased from −0.6 V to +0.5 V *vs* SCE. However, when the applied potential increased more, the photocurrent was only enhanced appreciably. Namely, the photocurrent almost reached a saturated value at +0.5 V *vs* SCE. Consequently, in further investigations of the photoelectrochemical degradation of 4-CP, +0.5 V *vs* SCE as the applied bias was selected.

The pollutants may undergo decomposition driven by electrolysis, photocatalysis and synergic photoelectrocatalysis in the photoelectrochemical system. The degradations of 4-CP, which is

Table 1
Products resulting from the photoelectrocatalytic degradation of 4-CP, observed as TMS derivatives by GC–MS (peak 3 was 4-CP with retention time of 9.90 min).

Peak no.	R. T. Min.	Intermediate	Formula weight	*m*/*z* values (relative abundance) EI
1	7.43	$HO_2C–CO_2H$	234	73 (27), 75 (29), 100 (6), 131 (5), 147 (100), 190 (31)
2	8.72	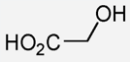	220	73 (62), 75 (22), 79 (12), 93 (24), 147 (100), 148 (16), 177 (12)
4	10.08	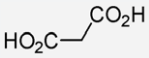	248	73 (25), 75 (8), 147 (100), 148 (17), 149 (9), 233 (5)
5	11.32		260	73 (36), 75 (9), 93 (24), 95 (8), 147 (100), 148 (17), 149 (9), 245 (8)
6	11.46	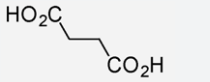	262	73 (25), 75 (10), 93 (6), 147 (100), 148 (17), 149 (9), 247 (10)
7	11.92	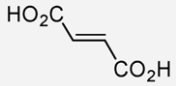	260	73 (38), 75 (20), 93 (27), 95 (10), 133 (8), 143 (21), 147 (50), 148 (9), 245 (100), 246 (20), 247 (10)
8	12.22	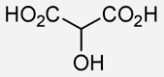	336	73 (89), 75 (18), 133 (7), 147 (100), 148 (9), 221 (6), 292 (12), 321 (6)
9	12.91	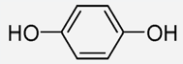	254	73 (82), 112 (10), 147 (6), 223 (7), 239 (91), 240 (19), 254 (100), 255 (24), 256 (10)
10	13.49	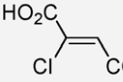	294	73 (80), 93 (25), 127 (28), 147 (23), 171 (5), 205 (6), 250 (5), 279 (100), 281 (35)
11	13.81	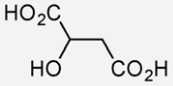	350	73 (100), 75 (32), 133 (7), 147 (77), 190 (12), 233 (22), 234 (5), 307 (5), 335 (11)
12	14.07	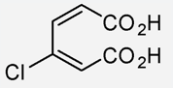	320	73 (100), 95 (15), 123 (25), 147 (98), 187 (10), 203 (70), 205 (24), 230 (10), 241 (10), 285 (50), 305 (20)
13	14.93	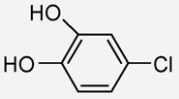	288	73 (100), 74 (10), 131 (5), 147 (4), 170 (9), 185 (8), 273 (7), 288 (52), 290 (20), 291 (5)
14	15.80	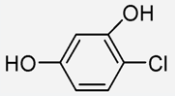	288	73 (100), 74 (15), 147 (8), 170 (11), 185 (4), 207 (15), 288 (63), 290 (25), 291 (8)
15	16.61	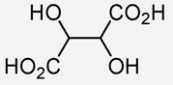	440	73 (100), 74 (8), 75 (11), 93 (6), 147 (66), 148 (10), 149 (7), 189 (7), 219 (7), 227 (5), 292 (13), 293 (7)

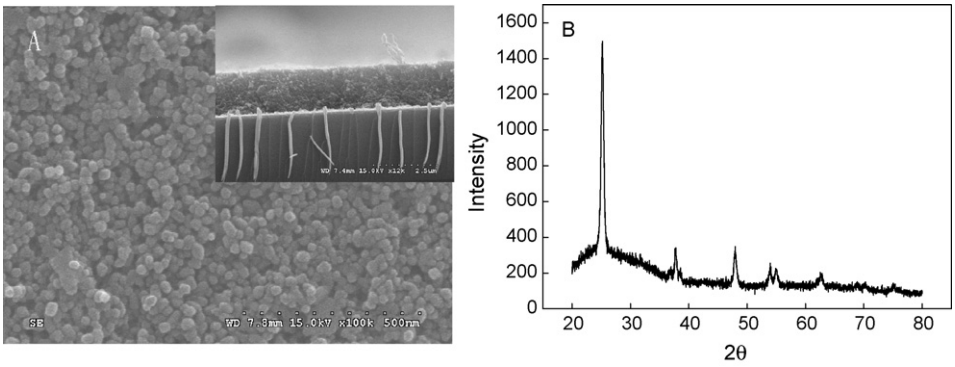

Fig. 1. (A) Surface images of TiO_2 film by SEM (the inset denotes the cross section of TiO_2 film); (B) XRD patterns of the TiO_2 film on SnO_2:F-coated glass substrates.

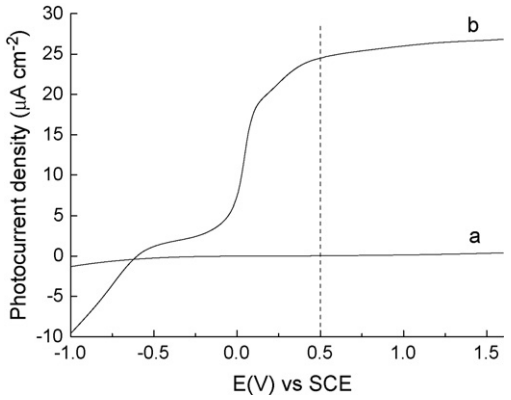

Fig. 2. Photocurrent–potential curves for TiO_2 thin-film electrode in 200 μM 4-CP (0.1 M Na_2SO_4, pH ≈ 5.8) solutions under dark condition (a) and UV irradiation (b). Scan rate = 10 mV s^{-1}.

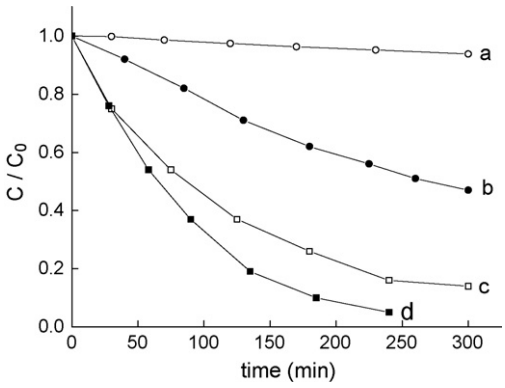

Fig. 3. Degradation of 4-CP (200 μM, pH ≈ 10) under different conditions: at a bias of 0.5 V in the dark (a); only under UV irradiation (b); under UV illumination and 0.5 V of bias potential (c) Ar-sparging; (d) O_2-saturated systems, respectively.

a representative aromatic contaminant, under various conditions were shown in Fig. 3.

When no external potential was applied, the UV illumination resulted in the degradation at a rate constant of about 2.75×10^{-3} min^{-1} (curve b), estimated by pseudo-first-order kinetic mode. When applied a potential of +0.5 V, direct electrochemical degradation of 4-CP without UV irradiation also exhibited slow rate constants of 7.49×10^{-4} min^{-1} (curve a). In absence of dissolved oxygen, about 86% of 4-CP was degraded when TiO_2 electrode was used as anode (+0.5 V), after 300 min of UV irradiation, and a much greater rate constant of 9.26×10^{-3} min^{-1} was observed (curve c). These results demonstrate the advantages of TiO_2-fim electrode and photoelectrocatalytic cell: (i) oxygen is not necessary to scavenge the photogenerated electrons since efficient charge separation of the photogenerated electrons and holes can be achieved by applying an anodic potential (+0.5 V) and (ii) the rate of degradation is enhanced by a factor of 3.4 as the applied anodic potential at +0.5 V *vs* SCE. Accordingly, there should be a synergistic effect between the electricity and radiation. The results are in agreement with Kamat et al. [29]. Correspondingly, the decomposition of 4-CP was also carried out in oxygen-saturated solution (curve d). After 240 min of UV illumination, 4-CP almost disappeared completely at a potential +0.5 V, and a more rate constant of 1.02×10^{-2} min^{-1} was obtained (curve d). Evidently, the rate constants of 4-CP degradation, with or without dissolved oxygen, are comparable to some extent for the photoelectrochemical system.

3.3. Determination of reaction by-products

The reaction intermediates of this photoelectrocatalytic process with immobilized TiO_2 films have now been analyzed to probe the reaction pathways in Ar-saturated and O_2-saturated solutions. The initial pH (unbuffered) of the solution was around 10. Solution of pH is one of the most important parameters that influence the photocatalytic reactions. Several researchers showed that the removal efficiency of chlorophenols decreased with increasing pH [30,31]. At acid pH values, the TiO_2 surface carries a net positive charge (pH_{zpc} 6.25), whereas chlorophenols and their intermediate products remain neutral or negatively charged. Therefore, acidic conditions facilitate the adsorption of the organic pollutants and enhance degradation. In contrast, better removal efficiency of chlorophenols in alkaline condition has also been reported [7,9,32,33]. It is explained that the higher pH can provide more hydroxide ions (OH^-) reacting with photo-holes to generate •OH radical, consequently enhancing the degradation rate of substituted phenols. Since the effect of pH cannot be generalized, Gogate and Pandit [34] recommended that laboratory scale studies are required for establishing the optimum pH unless data are available in the literatures with exactly similar operating conditions. In our case, the higher pH about 10 selected in the 4-CP photoelectrocatalytic degradation may be attributed to three reasons: (1) the transference of 4-CP and intermediates to the TiO_2 electrode is also possible on the effect of externally positive bias, although there is electrostatic repulsion between negative organic compounds and the TiO_2 surface at this pH; (2) more •OH radicals are formed at this pH with more OH^-; (3) more stable intermediates, especially acyclic acids, can be detected at the pH to explore the photocatalytic pathway, since acidic condition is more favorable for the mineralization of these acidic products [7,26].

The intermediates prior to the ring-opening stage detected by HPLC during the course of the degradation were hydroquinone, benzoquinone, catechol, 4-chlororesorcinol, and 4-chlorocatechol with retention times of 2.5, 3.2, 3.8, 5.9, and 10.1 min, respectively. The generation of these primary products mainly involves the addition of hydroxyl radicals to the organic substrate by three approaches of (a) hydroxylation of the aromatic ring, (b) substitution of chlorine by •OH, and (c) oxidation of hydroxylated hydroquinone to the corresponding benzoquinone. It is worth noting that although the intermediate hydroxyhydroquinone (1,2,4-phentriol) was expected prior to the destruction of the aromatic ring as reported by others [11,26], we were unable to detect this species by both GC–MS and HPLC techniques as attested by injection of an authentic sample of phentriol. It is likely that the volatility of this compound is too small to be eluted out under the gas chromatographic conditions used, and the polarity so great that it was eluted with the solvent phase in our HPLC analysis. Accordingly, we cannot preclude formation of phentriol in our systems.

Fig. 4 shows the kinetics of the disappearance of 4-CP in the presence of oxygen along with the formation and subsequent degradation of these hydroxylated intermediates in the working electrode compartment recorded at 280 nm by HPLC. A rapid degradation of 4-CP was seen at the TiO_2/TCO electrode which was held at an anodic potential of +0.5 V and irradiated with UV light. The initial photocurrent density was of the order 30 μA/cm^2 and decayed slowly during the operation of the cell due to the pH drop to 5. Nearly all of 4-CP disappeared within 4 h. The concentration of generated 4-chlorocatechol reached a maximum about 22.6 μM after 90 min irradiation, and subsequently decreased through its further decomposition. The concentration–time profiles of other intermediates observed were also similar to that of 4-chlorocatechol.

Breakdown of the aromatic ring results in the formation of a wide range of cleavage compounds such as low molecular weight carboxylic acids. To identify the compounds, GC–MS analysis was used, GC–MS analysis of the unfunctionalized degradation mixture

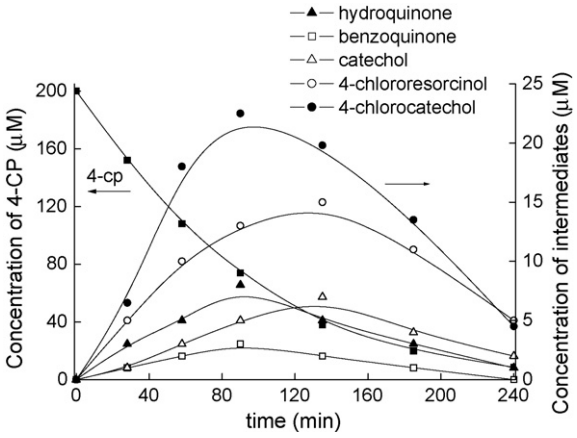

Fig. 4. Variations in the concentration of 4-CP and the hydroxylated products from the photoelectrocatalytic degradation of an oxygen-saturated aqueous solution of 4-CP (200 μM, pH ≈ 10) as a function of reaction time under UV illumination and 0.5 V of bias potential.

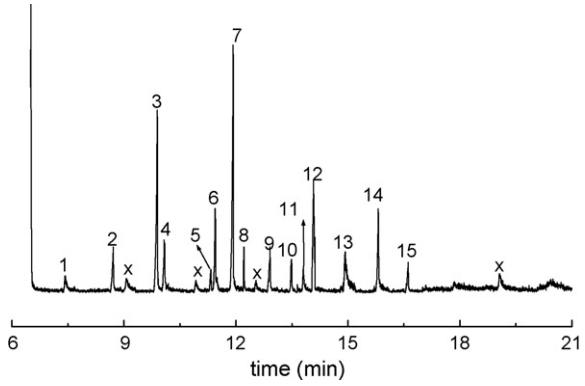

Fig. 5. Representative GC trace obtained on partial photoelectrocatalytic degradation of 4-CP (90 min) and silylation of the mixture. The peak numbers refer to the data in Table 1. The peak labeled "×" was not identified.

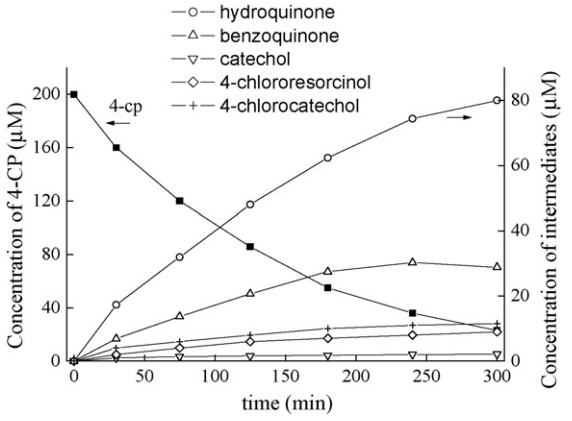

Fig. 6. Variations in the concentration of 4-CP and the hydroxylated intermediates from the photoelectrocatalytic degradation of an Ar-sparging aqueous solution of 4-CP (200 μM, pH ≈ 10) as a function of reaction time under UV illumination and 0.5 V bias potential.

was fruitless, no matter how it was processed, so the mixtures were silylated. Both alcohols and carboxylic acids were functionalized with TMS groups. In most instances, these structural assignments were confirmed with samples of authentic material that was processed in the same way that showed the same chromatographic and MS behavior. Fig. 5 indicated a representative trace for the silylated mixture of partial photoelectrocatalytic degradation of 4-CP. The data for the peaks of Fig. 5 were given in Table 1. All of the numbered peaks except those labeled "×" were identified with authentic compounds. Among of these aliphatic acids, peak 12 denotes 3-chloromuconic acid, which structure was confirmed by the authentic samples synthesized according to literature [27]. The six-carbon diacid is the most complicated product detected by GC–MS, which was formed through the cleavage of aromatic rings at the present experimental conditions. Therefore, under the combined effect of •OH radicals and dissolved oxygen, we deduced the formation of 3-chloromuconic acid by the opening ring of these hydroxylated intermediates is likely to be a main oxidation pathway. Subsequently, the intermediates of four-carbon and more low molecular weight were generated by further oxidating of 3-chloromuconic acid. However, other reasonable pathways also maybe exist to get to these compounds shown in Table 1.

The deoxidized experiments were carried out by continuously bubbling argon in the working electrode. The degradation rate of 4-CP decreased slightly (Fig. 3), but the nature of intermediates observed were similar to those obtained in the oxygen-saturated solution. Oppositely, it can be seen from Figs. 4 and 6 that the relative amounts of those intermediates were markedly different from the oxygen-saturated system. Pichat et al. have proposed that 4-CP undergoes degradation primarily to form HQ [35,36]. In air-equilibrated slurry reactions, they and others have observed the abundance of the intermediates detected in the relative proportion HQ ≫ BQ > 4-CC [37,38]. On the other hand, greater abundance of 4-CC as an intermediate has also been reported in the photocatalytically assisted and hydrogen peroxide mediated photodegradation of 4-CP [9,39–41]. Our results from these photoelectrocatalytic experiments indicate that, in argon-riched solutions, HQ is a major reaction intermediate while 4-CC predominates in oxygen-saturated case for the degradation of 4-CP. The difference in the

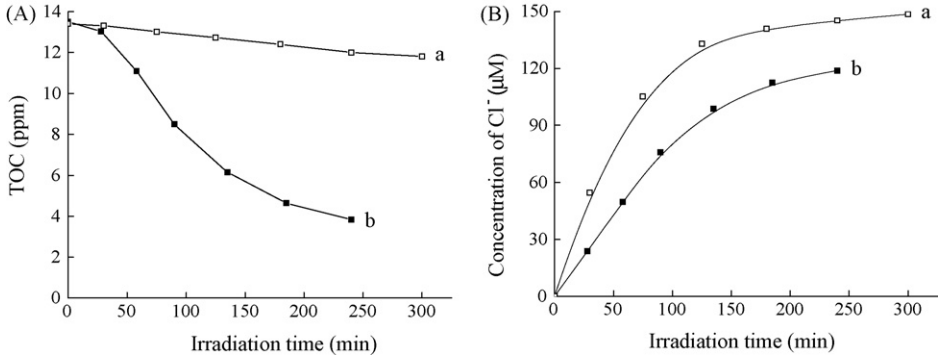

Fig. 7. Temporal changes in (A) total organic carbon (TOC) and (B) concentration of chloride ions in the degraded bulk solution during the photoelectrocatalytic degradation of 4-CP under UV illumination and 0.5 V (*vs* SCE) bias potential.

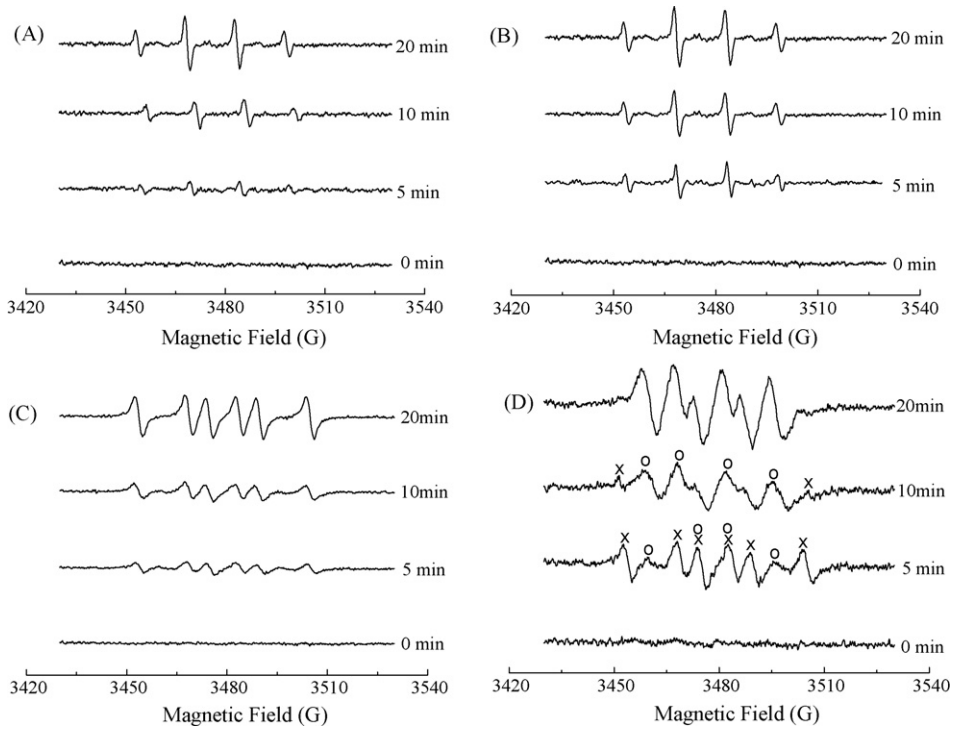

Fig. 8. DMPO spin-trap ESR spectra of TiO_2-film photoelectrochemical system without addition 4-CP under different conditions. (A) Signals detected in argon-sparging aqueous solution; (B) signals of oxygen bubbling aqueous solution; (C) signals examined in argon-sparging methanolic media and (D) signals of oxygen bubbling methanolic media, open circles placed above certain peak signals refer to ESR signals of the DMPO-peroxide adduct and the asterisks denote signals due to the DMPO-$HOCH_2$• adduct.

intermediates observed in O_2- and Ar-saturated solutions suggests that dissolved oxygen species play an important role in the course of 4-CP degradation. We attribute the indirect influence of O_2 on the reaction mechanism to two reasons: (i) oxygen plays a significant part in the further photocatalytic decomposition of hydroquinone and other hydroxylated intermediates; (ii) the presence of dissolved oxygen influences on the surface chemical processes.

Photocurrent measurements carried out in N_2- and O_2-saturated solutions have shown that oxygen adsorbs strongly on the surface of TiO_2 particles [15,42,43]. It is therefore proposed that, in oxygenated solutions, the affinity of oxygen for the TiO_2 surface displaces the poorly adsorbed 4-CP, depressing significantly its adsorption and dechlorination. However, in Ar-saturated solutions the surface chemical processes play a greater role leading to the formation of HQ. In traditional TiO_2 photocatalysis, the dechlorinated process of chlorophenols usually involves the following reactions: substitution of chlorine by •OH radical [7], photoreduction dechlorination [24] and direct photolysis [44]. For the present photoelectrocatalytic system, when a positive potential (+0.5 V) was applied to move photogenerated electrons, the dechlorination of 4-CP was mainly based on the •OH substitution by removal the chlorine at the *para*-position of benzene ring. Similarly, the intermediates generated in the absence of O_2 were also examined by GC–MS with the same way as the O_2-saturated case. Only a small quantity of oxalic acid was detected. These experimental results implied the mechanisms of subsequent oxidation for the primary hydroxylated products in the O_2- and Ar-saturated systems are greatly different.

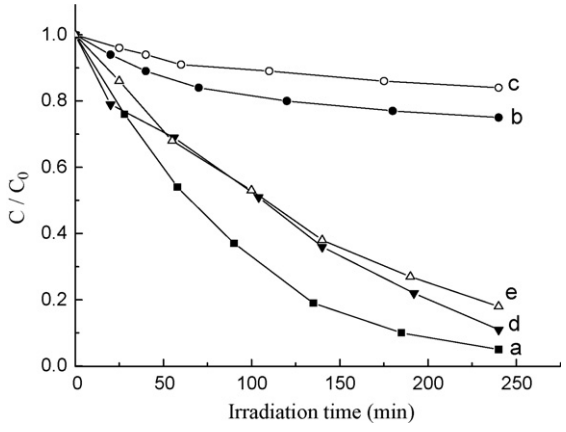

Fig. 9. Plotted degradation kinetics of 4-CP (200 μM, pH ≈ 10) under UV illumination and 0.5 V of bias potential in an oxygen-saturated solution on addition of (a) no scavenger added, (b) isopropanol, (c) methanol, (d) KH_2PO_4, (e) $NaHCO_3$. Scavenger concentration 0.1 M.

3.4. Mineralization and dechlorination

The extent of mineralization of 4-CP was examined by determination of both residual total organic carbon (TOC) and the quantity of inorganic chloride ions released. Temporal changes of TOC and variations in the concentration of chloride ion during the photoelectrodegradation process of 4-CP in the oxygen-saturated solution and in the Ar-sparging system were depicted in Fig. 7 (parts A and B, respectively).

The initial 4-CP (200 μM) contains 13.9 ppm of TOC. After the adsorption of 4-CP on the surface of TiO_2 electrode, the TOC values in the supernatants dropped slightly to 13.5 and 13.4 ppm for the O_2-bubbling and Ar-sparging systems, respectively. In the Ar-sparging case, TOC in the solution displayed limited and slow decrease during the irradiation period. In fact, less than 12% of TOC was removed after nearly 5 h of irradiation, indicating that mineralization of 4-CP occurred only to a slight extent under the conditions used. However, in the oxygen-saturated system, TOC decreased more than seven times faster relative to the Ar-sparging case (4.52×10^{-3} min^{-1} *vs* 5.76×10^{-4} min^{-1}). After a 4 h irradia-

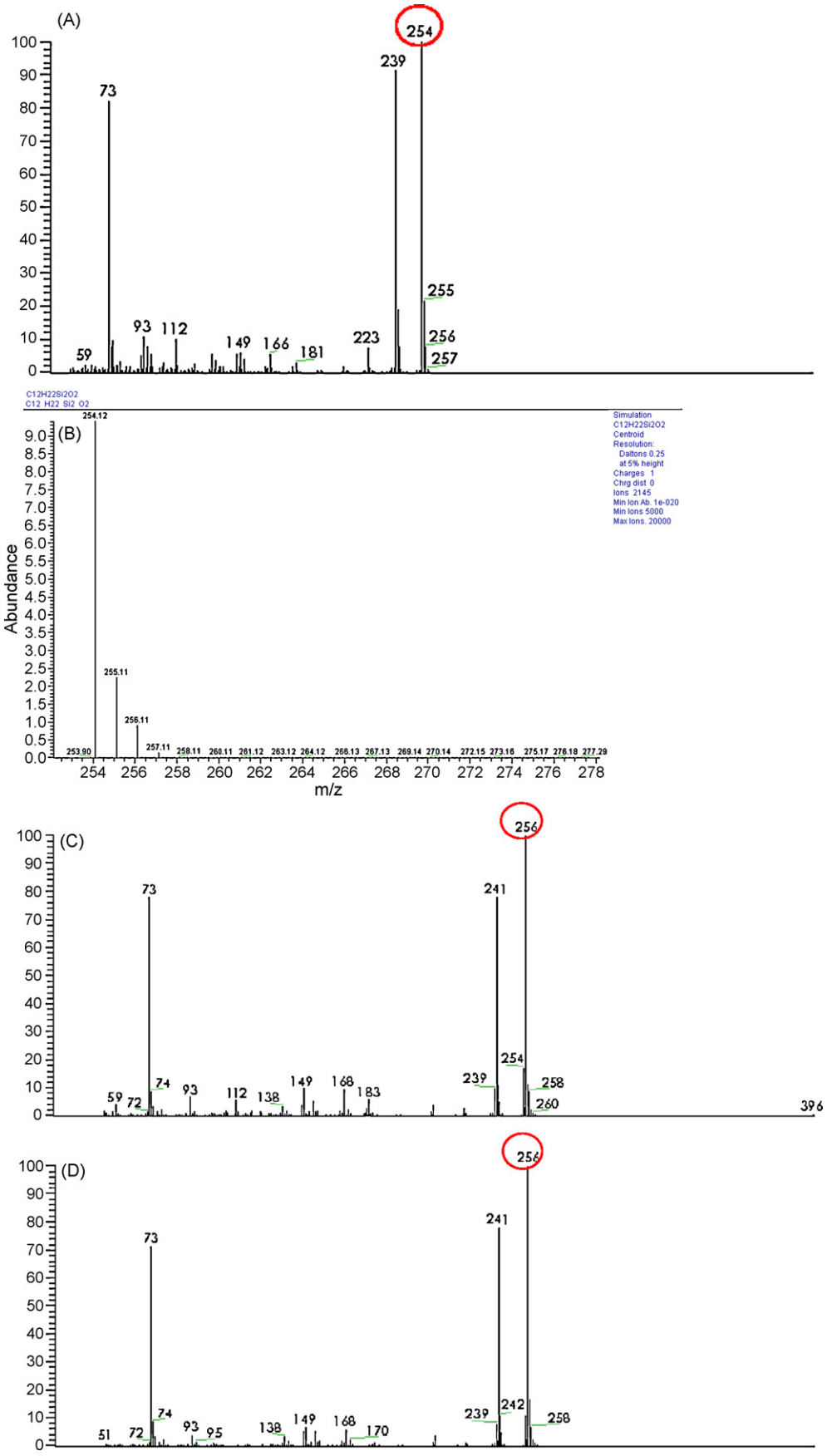

Fig. 10. (A) Observed EI mass spectra for the silylated derivative of hydroquinone ($C_{12}H_{22}Si_2O_2$) created in the photoelectrochemical degradation 4-CP; (B) computer-simulated parent peak and isotopic abundance patterns for $C_{12}H_{22}Si_2O_2$; (C) the EI mass spectrum of silylated hydroquinone generated in oxygen-saturated H_2O^{18} solution; (D) the EI mass spectrum of silylated hydroquinone yielded in argon-saturated H_2O^{18} solution; (E) corrected ion relative abundance of degradation products generated in the H_2O^{18} tracer experiments.

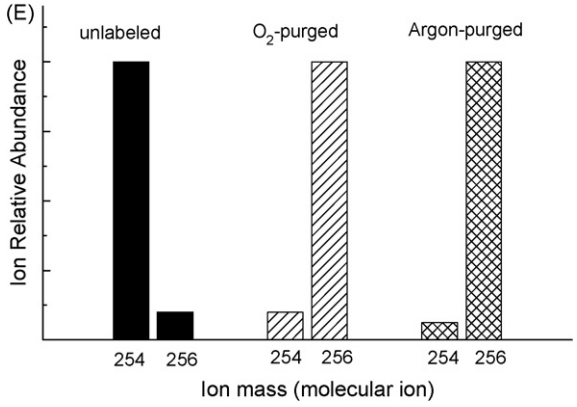

Fig. 10. (*Continued*).

tion period, ca. 72% of TOC was removed from the bulk solution in the oxygen-saturated condition. Relative to the TOC change, the release of chloride ions from the degradation of 4-CP occurred to a greater extent in both systems. The maximal extent of dechlorination was ca. 74% after 5 h of irradiation in the Ar-sparging solution (Fig. 7B, curve a), whereas in the oxygen-saturated system 60% of chloride ions were released after 4 h of irradiation (curve b).

3.5. Involved active species

ESR spectra of DMPO spin adducts were recorded following the same irradiation as used in the photoelectrochemical degradation of 4-CP. A spectrum displaying signals (Fig. 8A and B) with characteristic intensity 1:2:2:1 for DMPO-•OH adducts was obtained without addition 4-CP to the photoelectrochemical system, which indicated that the •OH radical was surely formed under the present conditions. It can be seen from Fig. 8A and B that the detected spectra of DMPO-•OH adducts in the presence or absence of dissolved oxygen were almost identical and the intensity of observed spectra increased gradually with irradiation time in the experimental range.

Additional examination for the generation and role of the •OH in the degradation of 4-CP came from effects of various scavengers of •OH radicals on the rate of 4-CP degradation, as indicated in Fig. 9. Since there was no significant amount of methanol and isopropanol absorbed on the catalyst in aqueous systems, they predominantly scavenged the free •OH radicals in solution. When they were introduced into the photoreaction system, the degradation of 4-CP was depressed drastically (curves b and c). However, inorganic anions usually inhibit the photodegradation of the pollutants by their trapping hydroxyl radicals [45–47]. Both $H_2PO_4^-$ and HCO_3^- have high adsorption on the surface of TiO_2. The adsorbed anions reacted with the positive holes and the adsorbed •OH on the surface of TiO_2. Addition of $H_2PO_4^-$ and HCO_3^- ions led to little suppression on the photodegradation rate of 4-CP (curves d and e). The results provided a solid indication that the free •OH radicals in solution were likely to be the main reactive species in the photoelectrocatalytic process.

It's known that the active oxygen species $O_2^{\bullet-}$ (or HOO• in acidic media) can be formed due to the reduction of oxygen by electrons from the conduction band of TiO_2 in dispersion system. To examine the capability of oxygen in trapping photogenerated electrons in the present photoelectrocatalytic cell, we also examined the radical signals yielded in methanolic media, which is advantageous to form the stable $O_2^{\bullet-}$ or HOO• radical. In the absence of dissolved oxygen, strong signals for the DMPO-$HOCH_2$• adduct emerged [48,49] and increased rapidly with illumination time. These signals (Fig. 8C) originate from attack of •OH radicals or photo-holes onto the CH_3OH molecules by H abstraction. However, the different radical signals were observed in the oxygen-saturated case. As shown in the Fig. 8D, the adduct spectra varied from a complex signals at 5 min to a simple radical spectrum after about 20 min, which is very analogous to that of DMPO-$O_2^{\bullet-}$ adduct. On the basis of signals in Fig. 8D, the predominant radical formed firstly was also $HOCH_2$• radical. Additionally, as very weak, another set of signals was detected at the early stage of irradiation. After that, this new signals was enhanced greatly with irradiation time. Previous studies [50,51] have reported that at high oxygen concentration, reaction of $HOCH_2$• with O_2 can quickly form stabilized $HOCH_2OO$• or HOO• radical by addition of oxygen to the carbon center or abstraction of hydrogen. Therefore, the radical signals generated subsequently in oxygen-saturated system, ascribed to these two peroxide radicals, if assuming they have similar ESR spectra.

3.6. Isotopic tracer experiments by using H_2O^{18}

In order to clarify the formation pathway of •OH radical in the present photoelectrochemical system, we have carried out the degradation experiments of 4-CP by using labeled H_2O^{18}. By the investigation percentage incorporation of O^{18} in the hydroxylated products, we obtained direct information of •OH radical. The isotopic tracer experiments were conducted in a pint-sized reactor, and the degradative mixture functionalized with silylation reagents was analyzed by GC–MS. Although the EI mass spectrograph of GC–MS employed in our experiments was not high resolution, it is adequate to analyze the isotopic percentage. The isotopic proportion of parent peak or fragment ion in the observed EI-MS matches excellently the simulated spectra using the Isotope Viewer software (version 1.0; in the Qual Browser of the Thermo Finnigan MS). Unfortunately, we were unable to detect the isotope peak of 4-chlorocatechnol and the detailed reason was unclear at present. By the detection of GC–MS, we obtained the intermediates peak of hydroquinone and aliphatic diacids, and their isotopic mass spectra. We have analyzed the isotopic data of hydroquinone mass spectra in detail.

In no isotope labeled experiment, the percentage of isotopic ion (m/z 256) in the hydroquinone was about 9.1% detected by EI mass spectra connected on the GC–MS (Fig. 10A), owing to the existence of natural isotope for Si, C and H elements, where the m/z 254 denoted the molecular ion of silylated derivative of hydroquinone ($C_{12}H_{22}Si_2O_2$). Computer-simulated parent peak and isotopic abundance patterns for $C_{12}H_{22}Si_2O_2$ was shown in Fig. 10B and the percentage of m/z 256 was 8.8%. It can be seen from these results the match between the observed and simulated spectra is excellent. In isotopic tracer experiment at oxygen-saturated solution, the percentage of m/z 256 was about 85.7% (Fig. 10C). Sim-

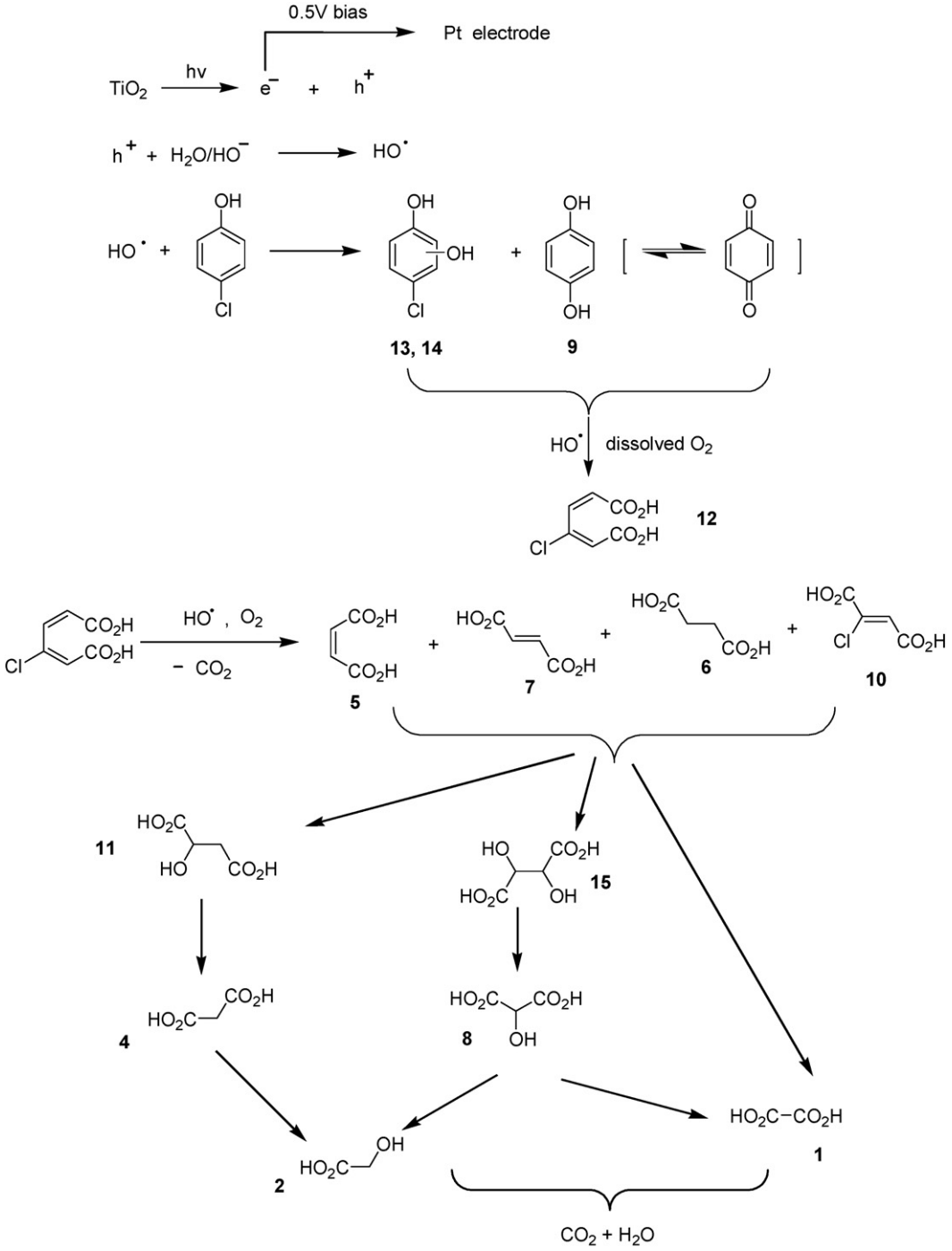

Scheme 2. Proposed mechanism of the photoelectrocatalytic degradation of 4-CP when applied a positive bias (+0.5 V) under UV illumination in the oxygen-saturated system.

ilarly, the content of m/z 256 was about 90.1%, generated in the argon-purged photoelectrochemical degradation (Fig. 10D). Taking account of the isotopic enrichment 85.6% of H_2O^{18} and the corporate effect of natural isotope of Si, C and H elements, we corrected the above experimental results (Fig. 10C and D), according to the following calculation formula. Finally, we gained the accurate percentage of m/z 256, which were indicated in Fig. 10E:

$$\frac{(\text{isotope abundance})_{\text{detected}} - (\text{natural abundance})_{\text{Si,H,C}}}{(\text{isotope percentage})_{H_2O^{18}}} \times 100\% \quad (9)$$

It is reported [52] by using H_2O^{18} that oxygen exchange between surface hydroxyl groups of TiO_2 and water in contact with it occurs quantitatively and rapidly in the dark at room temperature, whereas that between lattice oxygen and contacting water hardly occurs under the same conditions. This implies that, for TiO_2 in contact with H_2O^{18}, all surface hydroxyl groups are substituted by H_2O^{18}. From Fig. 10E, it can be seen that the corrected ratio of m/z 256 isotopic ion in hydroquinone derivative was about 93.6% in the argon-purged photoelectrochemical cell. The experimental result indicated that •OH radical was really formed by the photo-hole oxidation of surface hydroxyl ion and adsorbed water, not by photo-hole oxidation of surface lattice O atom. The percentage of m/z 256

isotope ion was about 88.7%, generated in the oxygen-saturated case, which is less than that of no oxygen system. The difference of m/z 256 isotopic ion (about 4.9%) is likely derived from the photoreduction of dissolved oxygen with conduction band electrons, though this formation pathway of $^{\bullet}OH$ radical is fairly minor in the present experiments.

3.7. Proposed mechanism

Absorption of UV light by TiO_2 nanoparticle results in charge separation. To avoid rapid charge recombination, a positive bias is usually applied to take away the photogenerated electrons in the electrochemically assisted TiO_2 photocatalysis. Because 4-CP is not strongly adsorbed to TiO_2 and the similarity of hydroxylated products obtained from photocatalytic degradation, the Fenton system and the hydrogen peroxide radiolysis [9,53,54], a rational assumption is made throughout this paper that all the photocatalytic reactions considered here begin with species related to the adsorbed hydroxyl radical.

Hydroxyl radical has a well-deserved reputation for addition reactions to aromatic rings, particularly on the position with high electron density. The product distributions detected by HPLC in the photocatalytic degradation of phenolic pollutants, such as phenol, 4-chlorophenol and 2,4-dichlorophenol [7,9,24] demonstrated assuredly that hydroxylation is the primary process. On the basis of data obtained by isotopic tracer experiments with H_2O^{18}, about 88.7% of the hydroxyl radicals which emerged in the hydroxylated intermediates originated from the oxidation H_2O or HO^- by valence band holes, even though at a high oxygen concentration.

Although a great amount of hydroxyl radical existing in an argon-saturated solution, mineralization did not undergo greatly in the photoelectrocatalytic degradation of 4-CP. It indicated that the enhancement in the separation efficiency of photogenerated charges and the concentration of hydroxyl radicals has little role in the opening of aromatic rings and mineralization. The similar results have been obtained in our earlier studies [24]. By loading the $PW_{12}{}^{3-}$ species on the surface of TiO_2, charge separation was improved significantly in the UV-illuminated TiO_2 due to electron transfer from the photo excited TiO_2 to $PW_{12}{}^{3-}$ species, thereby accelerating the hydroxylation of the initial 2,4-dichlorophenol substrate, but the mineralization of DCP was greatly suppressed in the presence of the polyoxomethalate.

The roles of O_2 in the photocatalytic degradations are twofold at least: (i) suppression of charge recombination by acting as an electron acceptor and (ii) participation in the chemical oxidative process of the substrates via active oxygen species. It is not clear for its specific role so far. The former function has been emphasized in the most previous investigations of TiO_2 mediated degradations. However, in the photoelectrochemical system, the role of oxygen, as an electron acceptor, is replaced by a positive bias potential. Therefore, the effect of oxygen mainly focuses on the direct participation in the chemical oxidative process of organic substrates. The obvious difference of mineralization yield between the oxygen-saturated and argon-purged photoelectrochemical degradation of 4-CP (Fig. 7A) suggested that dissolved oxygen, as an important oxidant, did take part in the opening of aromatic rings and mineralization. In addition, on the basis of aliphatic acids examined by GC–MS, the hydroxylated products of 4-CP were likely decomposed into aliphatic carboxylic acid and CO_2 *via* 3-chloromuconic acid, as shown in Scheme 2.

4. Conclusion

In summary, the photoelectrocatalysis provides an appropriate probe to reveal the reaction pathway of photocatalytic degradation of 4-CP under UV illumination. In this method, the effect of hydroxyl radical and oxygen species can be studied independently with the argon-sparging and oxygen-saturated system by applying a positive bias potential on TiO_2 electrode. The present results demonstrate (a) the active species $^{\bullet}OH$ is mainly formed by photohole oxidation of TiO_2 surface hydroxyl ion and adsorbed H_2O; (b) the hydroxylated products, via *cis, cis*-3-chloromuconic acid, were decomposed into aliphatic carboxylic acid and CO_2, which is likely to be a main degradation pathway; (c) dissolved oxygen species has an important role in the subsequent oxidation and mineralization of the intermediates of 4-chlorophenol.

Acknowledgements

This work was partially supported by the Key Technologies R&D Program of Henan Province (092102210364, 0624440034) and the Doctor Foundation of Henan Polytechnic University (B2008-58648265).

References

[1] M.R. Hoffmann, S.T. Martin, W.Y. Choi, D.W. Bahnemannt, Environmental applications of semiconductor photocatalysis, Chem. Rev. 95 (1995) 69–96.
[2] A.L. Linsebigler, G. Lu, J.T. Yates, Photocatalysis on TiO_2 surfaces: principles, mechanisms, and selected results, Chem. Rev. 95 (1995) 735–758.
[3] U.I. Gayaa, A.H. Abdullaha, Heterogeneous photocatalytic degradation of organic contaminants over titanium dioxide: a review of fundamentals, progress and problems, J. Photochem. Photobiol. C: Photochem. Rev. 9 (2008) 1–12.
[4] P. Oancea, T. Oncescu, The photocatalytic degradation of dichloros under solar irradiation, J. Photochem. Photobiol. A: Chem. 199 (2008) 8–13.
[5] A.B. Prevot, C. Baiocchi, M.C. Brussino, E. Pramauro, P. Savarino, V. Augugliaro, G. Marc, L. Palmisano, Photocatalytic degradation of Acid Blue 80 in aqueous solutions containing TiO_2 suspensions, Environ. Sci. Technol. 35 (2001) 971–976.
[6] K. Nagaveni, G. Sivalingam, M.S. Hegde, G. Madras, Photocatalytic degradation of organic compounds over combustion-synthesized nano-TiO_2, Environ. Sci. Technol. 38 (2004) 1600–1604.
[7] H. Liang, X. Li, Y. Yang, K.H. Sze, Effects of dissolved oxygen, pH, and anions on the 2,3-dichlorophenol degradation by photocatalytic reaction with anodic TiO_2 nanotube films, Chemosphere 73 (2008) 805–812.
[8] M. Kilic, Z. Cinar, Hydroxyl radical reactions with 4-chlorophenol as a model for heterogeneous photocatalysis, J. Mol. Struct. Theochem. 851 (2008) 263–270.
[9] U. Stafford, K.A. Gray, P.V. Kamat, Radiolytic and TiO_2-assisted photocatalytic degradation of 4-chlorophenol. A comparative study, J. Phys. Chem. 98 (1994) 6343–6351.
[10] C.C. Wong, W. Chu, The hydrogen peroxide-assisted photocatalytic degradation of alachlor in TiO_2 suspensions, Environ. Sci. Technol. 37 (2003) 2310–2316.
[11] J. Theurich, M. Lindner, D.W. Bahnemann, Photocatalytic degradation of 4-chlorophenol in aerated aqueous titanium dioxide suspensions: a kinetic and mechanistic study, Langmuir 12 (1996) 6368–6376.
[12] R. Nakamura, Y. Nakato, Primary intermediates of oxygen photoevolution reaction on TiO (rutile) particles, revealed by in situ FTIR absorption and photoluminescence measurements, J. Am. Chem. Soc. 126 (2004) 1290–1298.
[13] P. Salvador, On the nature of photogenerated radical species active in the oxidative degradation of dissolved pollutants with TiO aqueous suspensions: a revision in the light of the electronic structure of adsorbed water, J. Phys. Chem. C 111 (2007) 17038–17043.
[14] A. Fujishima, K. Honda, Photolysis-decomposition of water at the surface of an irradiated semiconductor, Nature 238 (1972) 37–38.
[15] K. Vinodgopal, S. Hotchandani, P.V. Kamat, Electrochemically assisted photocatalysis: titania particulate film electrodes for photocatalytic degradation of 4-chlorophenol, J. Phys. Chem. 97 (1993) 9040–9044.
[16] J. Li, L. Zheng, L. Li, Y. Xian, L. Jin, Fabrication of TiO_2/Ti electrode by laser-assisted anodic oxidation and its application on photoelectrocatalytic degradation of methylene blue, J. Hazard. Mater. B 139 (2007) 72–78.
[17] M.E. Calvo, R.J. Candal, S.A. Bilmes, Photooxidation of organic mixtures on biased TiO_2 films, Environ. Sci. Technol. 35 (2001) 4132–4138.
[18] K. Vinodgopal, I. Bedja, P.V. Kamat, Nanostructured semiconductor films for photocatalysis: photoelectrochemical behavior of SnO_2/TiO_2 composite systems and its role in photocatalytic degradation of a textile azo dye, Chem. Mater. 8 (1996) 2180–2187.
[19] D.H. Kim, M.A. Anderson, Photoelectrocatalytic degradation of formic acid using a porous titanium dioxide thin-film electrode, Environ. Sci. Technol. 28 (1994) 479–485.
[20] J.M. Kesselman, N.S. Lewis, M.R. Hoffman, Photoelectrochemical degradation of 4-chlorocatechol at TiO_2 electrodes: comparison between sorption and photoreactivity, Environ. Sci. Technol. 31 (1997) 2298–2302.

[21] X. Li, F. Li, C. Fan, Y. Sun, Photoelectrocatalytic degradation of humic acid in aqueous solution using a Ti/TiO_2 mesh photoelectrode, Water Res. 36 (2002) 2215–2224.
[22] T. Ruzgas, J. Emneus, L. Gorton, V.G. Marko, The development of a peroxidase biosensor for monitoring phenol and related aromatic compounds, Anal. Chem. Acta 31 (1995) 245–253.
[23] M.P. Titius, V.G. Molina, M. Banos, J. Gimenez, S. Esplugas, Degradation of chlorophenols by means of advanced oxidation processes: a general review, Appl. Catal. B 47 (2004) 219–256.
[24] C. Chen, P. Lei, H. Ji, W. Ma, J. Zhao, Photocatalysis by titanium dioxide and polyoxometalate/TiO_2 cocatalysts. Intermediates and mechanistic study, Environ. Sci. Technol. 38 (2004) 329–337.
[25] J. Yang, C. Chen, H. Ji, Mechanism of TiO_2-assisted photocatalytic degradation of dyes under visible irradiation: photoelectrocatalytic study by TiO_2-film electrodes, J. Phys. Chem. B 109 (2005) 21900–21905.
[26] X. Li, J.W. Cubbage, T.A. Tetzlaff, W.S. Jenks, Photocatalytic degradation of 4-chlorophenol. 1. The hydroquinone pathway, J. Org. Chem. 64 (1999) 8509–8524.
[27] S.R. Kaschabek, W. Reineke, Synthesis of bacterial metabolites from haloaromatic degradation. 1. Fe(III)-catalyzed peracetic acid oxidation of halocatechols, a facile entry to cis,cis-2-halo-2,4-hexadienedioic acids and 3-halo-5-oxo-2(5H)-furanylideneacetic acids, J. Org. Chem. 59 (1994) 4001–4003.
[28] G. Rothenberger, D. Fitzmaurice, M. Gratzel, Spectroscopy of conduction band electrons in transparent metal oxide semiconductor films: optical determination of the flatband potential of colloidal titanium dioxide films, J. Phys. Chem. 96 (1992) 5983–5986.
[29] K. Vinodgnpa1, U. Stafford, K.A. Gray, P.V. Kamat, Electrochemically assisted photocatalysis. 2. The role of oxygen and reaction intermediates in the degradation of 4-chlorophenol on immobilized TiO_2 particulate films, J. Phys. Chem. 98 (1994) 6797–6803.
[30] Y. Ku, R.M. Leu, K.C. Lee, Decomposition of 2-chlorophenol in aqueous solution by UV irradiation with the presence of titanium dioxide, Water Res. 30 (1996) 2569–2578.
[31] X. Quan, X. Ruan, H. Zhao, S. Chen, Y. Zhao, Photoelectrocatalytic degradation of pentachlorophenol in aqueous solution using a TiO_2 nanotube film electrode, Environ. Pollut. 147 (2007) 409–414.
[32] N. Serpone, P. Maruthamuthu, P. Pichat, E. Pelizzetti, H. Hidaka, Exploiting the interparticle electron transfer process in the photocatalyzed oxidation of phenol, 2-chlorophenol and pentachlorophenol: chemical evidence for electron and hole transfer between coupled semiconductors, J. Photochem. Photobiol. A 85 (1995) 247–255.
[33] R. Doong, C. Chen, R. Maithreepala, S. Chang, The influence of pH and cadmium sulfide on the photocatalytic degradation of 2-chlorophenol in titanium dioxide suspensions, Water Res. 35 (2001) 2873–2880.
[34] P.R. Gogate, A.B. Pandit, A review of imperative technologies for wastewater treatment I: oxidation technologies at ambient conditions, Adv. Environ. Res. 8 (2004) 501–551.
[35] J.C. D'Oliveira, G.A. Sayyed, P. Pichat, Photodegradation of 2- and 3-chlorophenol in TiO_2 aqueous suspensions, Environ. Sci. Technol. 24 (1990) 990–996.
[36] G.A. Sayyed, J.C. D'Oliveira, P. Pichat, Semiconductor-sensitized photodegradation of 4-chlorophenol in water, J. Photochem. Photobiol. A: Chem. 58 (1991) 99–113.
[37] N. Serpone, R. Terzian, H. Hidaka, E. Pelizzetti, Ultrasonic induced dehalogenation and oxidation of 2-, 3-, and 4-chlorophenol in air-equilibrated aqueous media. Similarities with irradiated semiconductor particulates, J. Phys. Chem. 98 (1994) 2634–2640.
[38] E. Leyva, E. Moctezuma, M.G. Ruiz, L.T. Martinez, Photodegradation of phenol and 4-chlorophenol by BaO-Li_2O-TiO_2 catalysts, Catal. Today 40 (1998) 367–376.
[39] A. Mills, S. Morris, R. Davies, Photomineralization of 4-chlorophenol sensitised by titanium dioxide: a study of the intermediates, J. Photochem. Photobiol. A: Chem. 70 (1993) 183–189.
[40] A. Mills, S. Moms, Photomineralisation of 4-chlorophenol sensitised by titanium dioxide: a study of the effect of annealing the photocatalyst at different temperatures, J. Photochem. Photobiol. A: Chem. 71 (1993) 285–289.
[41] A. Mills, P. Sawunyama, Photocatalytic degradation of 4-chlorophenol mediated by TiO_2: a comparative study of the activity of laboratory made and commercial TiO_2 samples, J. Photochem. Photobiol. A: Chem. 84 (1994) 305–309.
[42] H. Gerischer, Photoelectrochemical catalysis of the oxidation of organic molecules by oxygen on small semiconductor particles with TiO_2 as an example, Electrochim. Acta 38 (1993) 3–9.
[43] C. Wang, A. Heller, H. Gerischer, Palladium catalysis of O_2 reduction by electrons accumulated on TiO_2 particles during photoassisted oxidation of organic compounds, J. Am. Chem. Soc. 114 (1992) 5230–5234.
[44] M. Czaplicka, A. Czaplicki, Photodegradation of 2,3,4,5-tetrachlorophenol in water/methanol mixture, J. Photochem. Photobiol. A: Chem. 178 (2006) 90–97.
[45] K. Wang, J. Zhang, L. Lou, S. Yang, Y. Chen, UV or visible light induced photodegradation of AO7 on TiO_2 particles: the influence of inorganic anions, J. Photochem. Photobiol. A: Chem. 165 (2004) 201–207.
[46] C. Hu, X. Hu, L. Wang, J. Qu, A. Wang, Visible-light induced photocatalytic degradation of azodyes in aqueous AgI/TiO_2 dispersion, Environ. Sci. Technol. 40 (2006) 7903–7907.
[47] P.F. Schwarz, N.J. Turro, A new method to determine the generation of hydroxyl radicals in illuminated TiO_2 suspensions, J. Phys. Chem. B 101 (1997) 7127–7134.
[48] T. Wu, T. Lin, J. Zhao, H. Hidaka, N. Serpone, TiO_2-assisted photodegradation of dyes. 9. Photooxidation of a squarylium cyanine dye in aqueous dispersions under visible light irradiation, Environ. Sci. Technol. 33 (1999) 1379–1387.
[49] T. Wu, G. Liu, J. Zhao, H. Hidaka, N. Serpone, Mechanism study of the TiO_2-assisted photodegradation of squarylium cyanine dye in methanolic suspensions exposed to visible light, New J. Chem. 24 (2000) 93–98.
[50] C. Anastasi, M. Broomfield, O.J. Nielsen, P. Pagsberg, Kinetics and mechanisms of the reactions of mercaptomethyl radicals with dioxygen, nitric oxide, and nitrogen dioxide, J. Phys. Chem. 96 (1992) 696–701.
[51] T.J. Wallington, P. Dagaut, M.J. Kurylo, UV absorption cross sections and reaction kinetics and mechanisms for peroxy radicals in the gas phase, Chem. Rev. 92 (1992) 667–710.
[52] S. Sato, Hydrogen and oxygen isotope exchange reactions over illuminated and nonilluminated titania, J. Phys. Chem. 91 (1987) 2895–2897.
[53] F. Mijangos, F. Varona, N. Villota, Changes in solution color during phenol oxidation by Fenton reagent, Environ. Sci. Technol. 40 (2006) 5538–5543.
[54] J.A. Zazo, J.A. Casas, A.F. Mohedano, M.A. Gilarranz, J.J. Rodriguez, Chemical pathway and kinetics of phenol oxidation by Fenton's reagent, Environ. Sci. Technol. 39 (2005) 9295–9300.